Human Pathology (2019) **85**, 210–220

ELSEVIER

Human PATHOLOGY

www.elsevier.com/locate/humpath

Original contribution

Immunophenotypic profile as a predictor of prognosis in advanced ovarian carcinoma☆,☆☆

Ako Yokoi BPh[a], Toshihide Matsumoto PhD[a], Go Watanabe PhD[b], Masataka Tochimoto MD[a], Makoto Saegusa MD, PhD[a,*]

[a]*Department of Pathology, Kitasato University School of Medicine, Sagamihara, Kanagawa 252-0374, Japan*
[b]*Department of Biophysics, School of Science, Kitasato University, Sagamihara, Kanagawa 252-0374, Japan*

Received 13 August 2018; revised 20 October 2018; accepted 31 October 2018

Keywords:
Ovarian carcinoma;
Immunohistochemical profile;
Prognosis;
p53;
HNF-1β;
ARID1A

Summary Although proteomic profiles for ovarian epithelial carcinoma (OECa) have been widely investigated, no single marker or set of predictors has been clinically implemented mainly because their reliability and validity have not yet been well established. To establish immunohistochemical (IHC) panels for prognosis prediction of OECa for use in daily pathology practice, the expression patterns of 12 IHC markers, p53, HNF-1β, ARID1A, estrogen receptor-α, progesterone receptor, vimentin, PTEN, PIK3CA, WT1, left-right determination factor, β-catenin, and Ki-67 were investigated using 282 OECas. Hierarchical clustering analysis revealed 7 major immunoprofile groups (IPGs I-VII) that could be used to categorize OECa tumors independent of histotypes. Based on the results of the cluster analysis and protein expression statuses, we further demonstrated the effective classification of OECa tumors into simplified immunoprofile panels using only 4 IHC markers including HNF-1β, p53, ARID1A, and WT1. The tumors in IPG VII with HNF1β+/p53+/ARID1A+ immunophenotype demonstrated a significantly worse overall survival and progression-free survival as compared with the other IPGs. Multivariate Cox regression analysis also revealed that the immunophenotype (HNF1β+/p53+/ARID1A+) and clinical stage were significant and independent prognostic factors for overall survival and progression-free survival in advanced OECa. In conclusion, we identified immunoprofiles in OECa using a panel of 4 IHC markers, which could identify tumors by the immunophenotype that is associated with the most unfavorable prognosis and thus facilitate prognosis prediction of advanced OECa.

1. Introduction

Ovarian epithelial carcinoma (OECa), which is divided into 5 major histologic subtypes including high-grade serous (HGSeCa), low-grade serous (LGSeCa), endometrioid (EmCa), clear cell (CCCa), and mucinous carcinomas (MuCa), is the most deadly group of gynecologic malignancies in Japan [1]. The major reason for the poor prognosis is late diagnosis; more than 75% of patients are diagnosed as having advanced-stage disease characterized by metastasis to the peritoneal cavity

☆ Competing interests: Potential conflicts do not exist.

☆☆ Funding/Support: This study was supported by a grant from JSPS KAKENHI (Grant No. 17K08703).

* Corresponding author at: Department of Pathology, Kitasato University School of Medicine, 1-15-1 Kitasato, Minami-ku, Sagamihara, Kanagawa 252-0374, Japan.

E-mail addresses: am12104@st.kitasato-u.ac.jp (A. Yokoi), matsumoto@med.kitasato-u.ac.jp (T. Matsumoto), go0325@kitasato-u.ac.jp (G. Watanabe), m-tochi@med.kitasato-u.ac.jp (M. Tochimoto), msaegusa@med.kitasato-u.ac.jp (M. Saegusa).

https://doi.org/10.1016/j.humpath.2018.10.036
0046-8177/

[1-4]. Recently, OECa is considered a heterogeneous group of carcinomas with remarkable differences in pathobiology and tumor behavior, on the basis of several molecular biological findings [5].

Although classic clinicopathological factors, such as age, stage, residual tumor after first laparotomy, differentiation grade, histotype, and response to chemotherapy, are important prognostic markers for OECa, it is not possible to determine optimal chemotherapy on an individual patient basis according to these factors [6,7]. However, studies have shown that biomarker profiling using tumor tissues, cell lines, ascites fluid, and blood samples from OECa patients may help predict patient response to available treatment or prognosis [8-11], but no single marker or set of genes with predictive value has been clinically implemented mainly because their reliability and validity have not yet been well established [7].

OECas of different histotypes show different responses to conventional chemotherapy; thus, there has been interest in subtype-specific treatment of the tumors [12,13]. However, histotypic diagnosis by pathologists has been only modestly reproducible [14-16]; the concordance rates of interobserver reproducibility have been reported to be from 56% to 68%, with κ statistics of 0.46 to 0.55. In contrast, ancillary examinations such as immunohistochemistry (IHC) for specific markers can increase reproducibility [17,18], suggesting that the detection of several IHC markers, such as p53, HNF-1β, vimentin, WT1, p16, and Ki-67, which have all been shown to be associated with the different histotypes of OECas [13], may assist in identifying the different subtypes of OECas. Alternatively, IHC examination may be useful for determination of subtype-specific treatment of OECa. In this study, we investigated the expression patterns of 12 protein markers, p53, HNF-1β, ARID1A, estrogen receptor-α (ERα), progesterone receptor (PR), vimentin, PTEN, PIK3CA, WT1, left-right determination factor (LEFTY), β-catenin, and Ki-67, by IHC in 282 cases of OECa and demonstrated that the tumors could be categorized into 7 immunoprofile groups (IPGs) using hierarchical clustering. In addition, we developed a simplified categorization system of OECa cases into the IPGs using the 4 most useful IHC markers, which could facilitate the prediction of the behavior of advanced OECa.

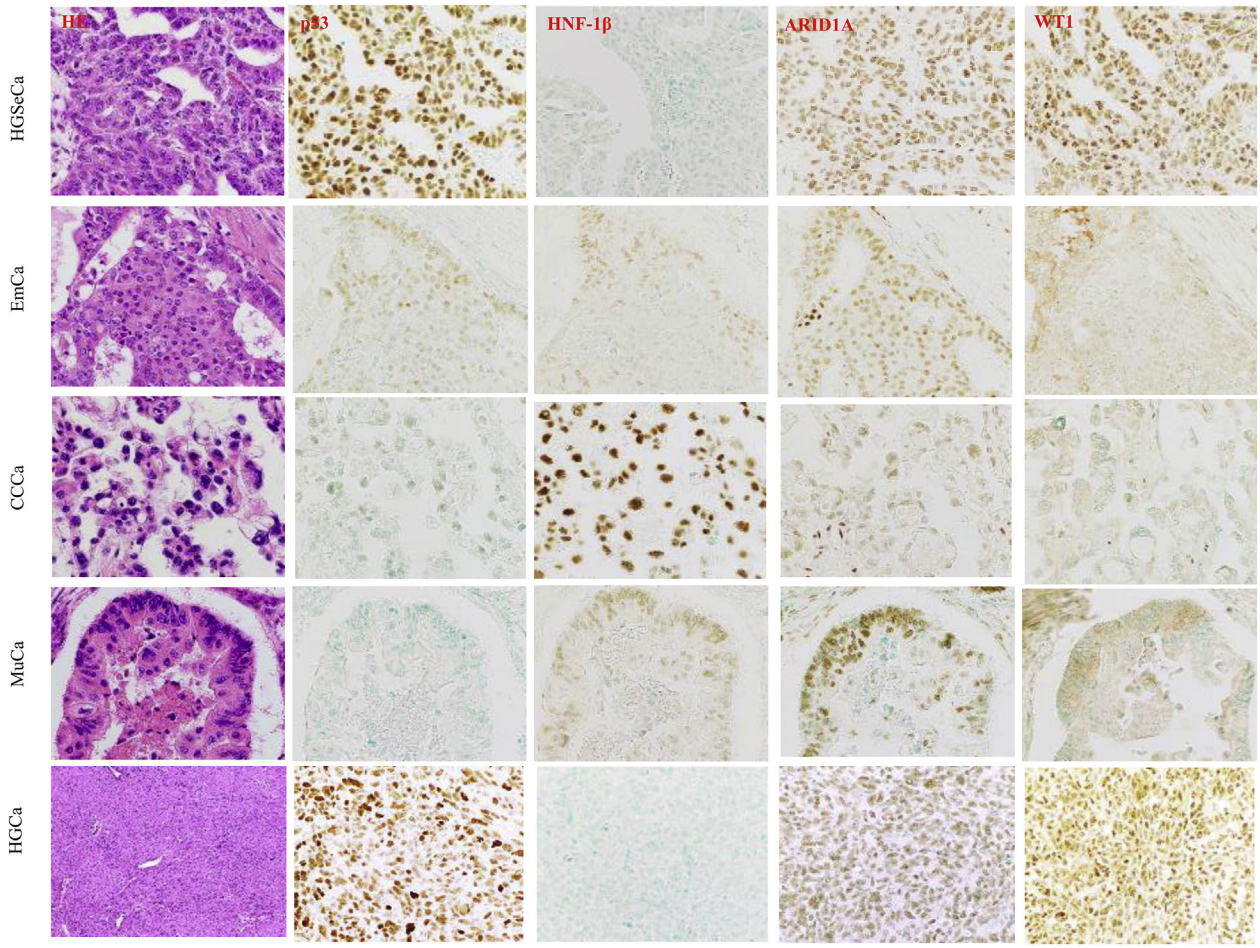

Fig. 1 IHC findings in OECa. Staining by hematoxylin and eosin and IHC for the 4 most correlative markers, p53, HNF-1β, ARID1A, and WT1, in OECas tissues including HGSeCa, EmCa, CCCa, MuCa, and HGCa. Original magnification ×200.

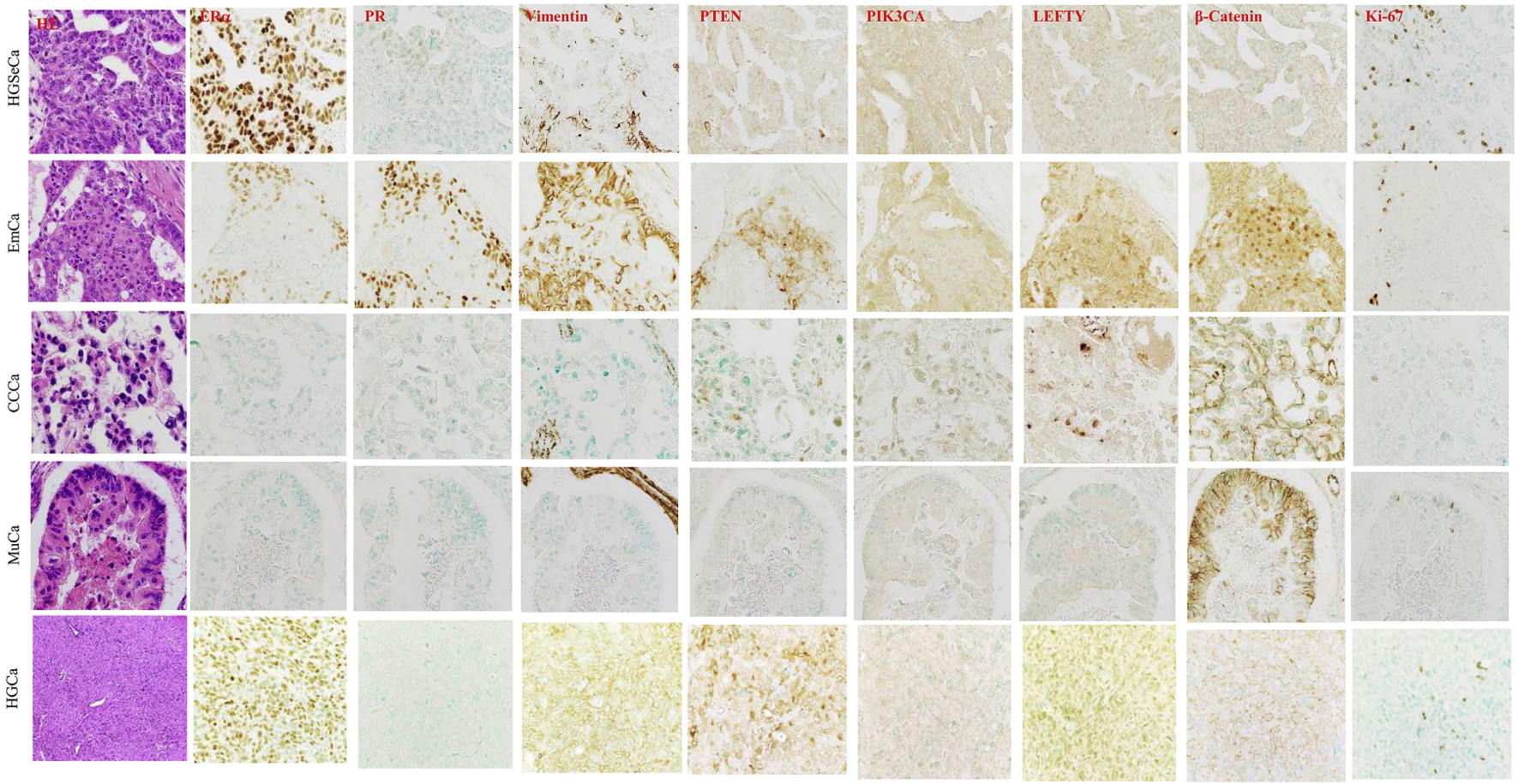

Fig. 2 IHC findings in OECa. Staining by hematoxylin and eosin and IHC for 8 protein markers, ERα, PR, vimentin, PTEN, PIK3CA, LEFTY, β-catenin, and Ki-67, in OECas tissues including HGSeCa, EmCa, CCCa, MuCa, and HGCa. Original magnification ×200.

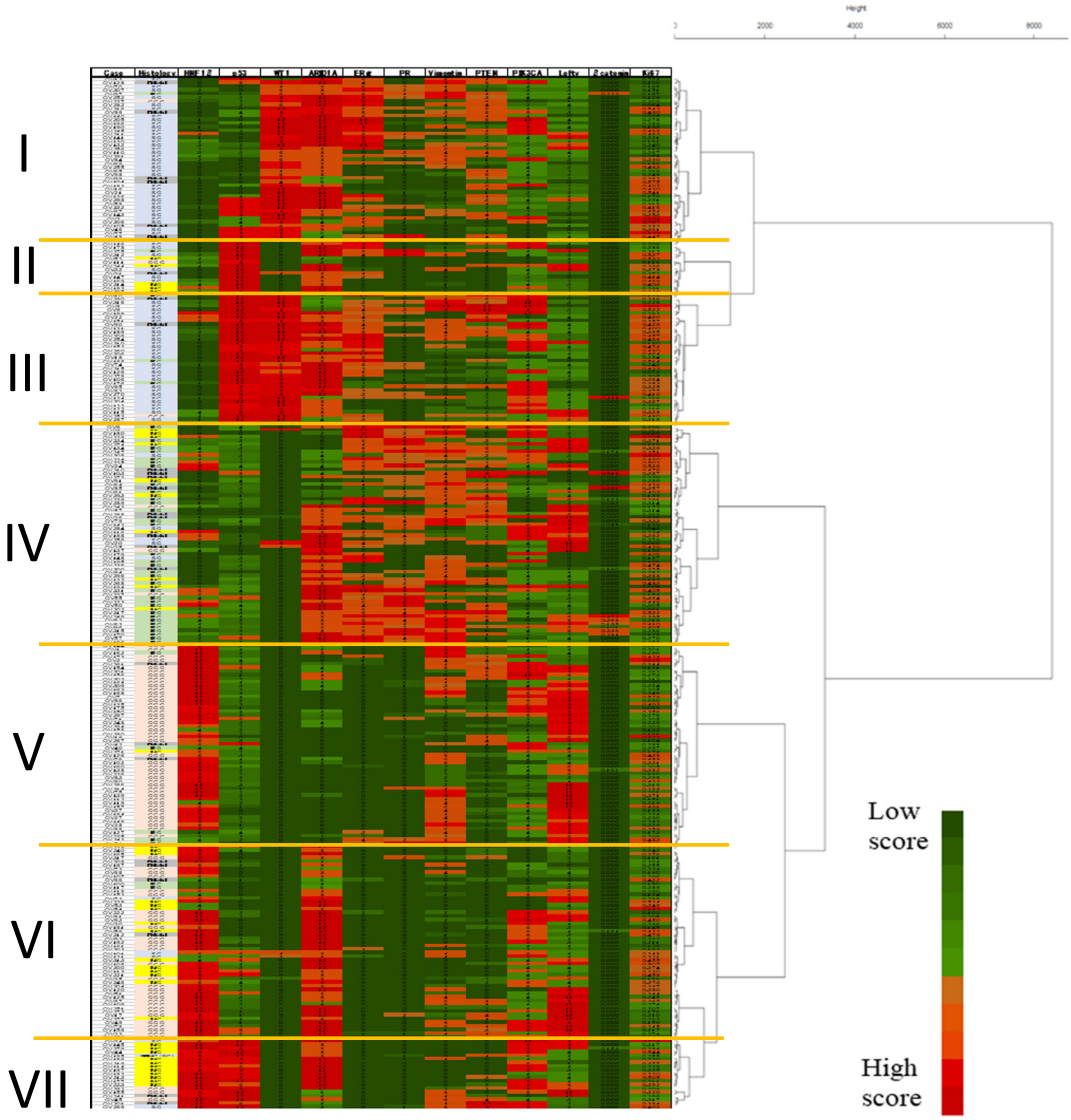

Fig. 3 Unsupervised hierarchical clustering of OECas. The expression level of each protein is colored; red, orange, and green indicate relatively high (IHC scores or LIs > means + SDs), neutral (means ± SDs), and low (< means − SDs) expression, respectively. Major clusters are shown as IPGs I to VII.

Table 1 Relationship between IPGs and histotypes in OECa

IPG	n	Histotype					
		HGSeCa, n (%)	LGSeCa, n (%)	EmCa, n (%)	CCCa, n (%)	MuCa, n (%)	HGCa, n (%)
I	38	18 (47.4)	11 (28.9)	2 (5.3)	1 (2.3)	1 (2.6)	5 (13.2)
II	18	6 (33.3)	1 (5.6)	4 (22.2)	1 (6.7)	5 (33.3)	1 (6.7)
III	42	32 (76.2)	1 (2.4)	3 (8.6)	1 (2.9)	0 (0)	5 (11.9)
IV	54	2 (3.7)	0	31 (57.4)	6 (11.1)	9 (16.7)	6 (11.1)
V	57	2 (3.5)	0	2 (3.5)	44 (77.2)	2 (3.5)	7 (12.3)
VI	47	3 (5.7)	0	5 (10.6)	27 (57.4)	9 (19.1)	6 (6.4)
VII	26	6 (23.1)	0	0 (0)	5 (19.2)	15 (57.7)	0 (0)

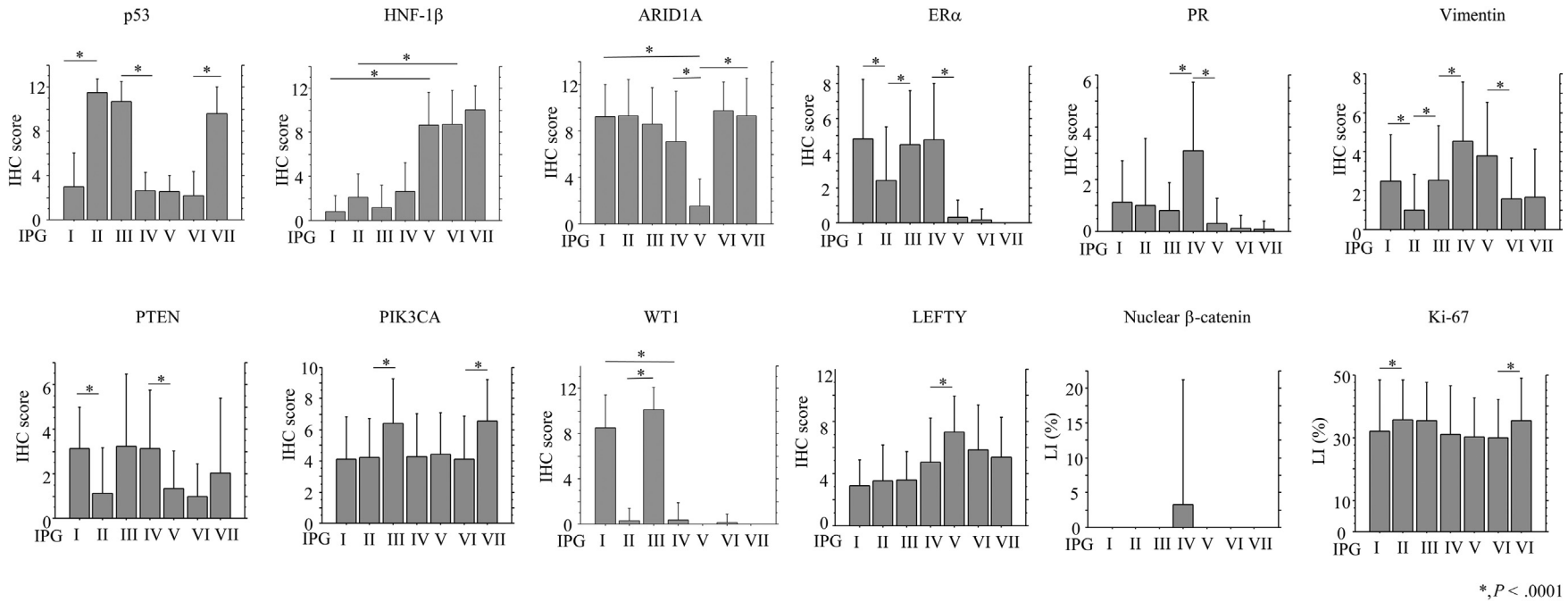

Fig. 4 Relationship of the IHC scores for the 12 protein markers with IPGs in OECa. The data shown are means ± SDs.

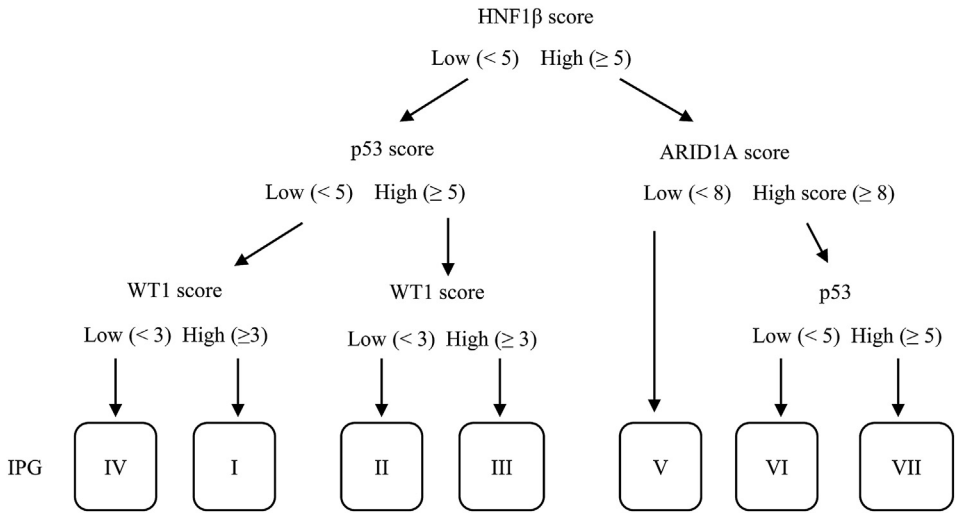

Fig. 5 Flowchart to categorize OECa cases into the 7 IPGs using the 4 most correlative IHC markers including HNF-1β, p53, ARID1A, and WT1. The high and low categories represent the expression level of each marker on the basis of the mean cutoff values.

2. Materials and methods

2.1. Clinical cases

A total of 282 cases of OECas, surgically resected at Kitasato University Hospital in the period from 2006 to 2015, were selected from our patient records according to the criteria of the 2014 World Health Organization classification [19]. All patients underwent oophorectomy with or without hysterectomy. None of the patients had received chemotherapy or any other treatment preoperatively. The histopathologic diagnosis for ovarian carcinomas with a typical histology was usually conducted using only hematoxylin and eosin–based examination, whereas the diagnosis for tumors with an atypical feature was determined by the IHC approach using a few antibodies, such as HNF-1β, WT-1, and hormone receptors. The tumor cases investigated comprised 69 HGSeCas, 13 LGSeCas, 47 EmCas, 85 CCCas, and 41 MuCas, as well as 27 high-grade carcinomas (HGCas) that showed a lack of histotype-specific differentiation features. Detailed clinical and pathological information was investigated by A. Y. and T. M. using our patient record. Briefly, the mean age of the patients was 57 years (range, 25-89 years). The average tumor size was 11 cm (range, 1-30 cm). According to the criteria of the International Federation of Gynecology and Obstetrics (FIGO) [20], 108 cases were subcategorized as stage I and 153 as stage II to IV. Forty-three cases were positive for nodal metastasis, whereas 178 were negative. In addition, 21 cases showed distant metastasis in contrast to 261 that were negative. All tissues were routinely fixed in 10% formalin and processed for embedding in paraffin wax. Approval for this study was given by the Ethics Committee of the Kitasato University School of Medicine (B16-10).

2.2. Antibodies

Anti–β-catenin and anti–HNF-1β antibodies were bought from BD Biosciences (San Jose, CA). Anti-WT1, antivimentin, anti-p53, and anti–Ki-67 antibodies were purchased from Dako (Copenhagen, Denmark). Anti-ERα and anti-PR antibodies were from Novocastra (Newcastle, United Kingdom). Anti-PIK3CA, anti-LEFTY, anti-ARID1A, and anti-PTEN antibodies were from Cell Signaling Technology (Danvers, MA), Abcam (Cambridge, MA), Sigma-Aldrich Chemicals (St Louis, MO), and Millipore (Temecula, CA), respectively.

2.3. Immunohistochemistry

IHC was performed using a combination of the microwave-oven heating and polymer immunocomplex (Envision, Dako) methods using whole sections. Briefly, after ordinary deparaffinization of 4-μm-thick sections, endogenous peroxidase was blocked by treatment of 0.3% hydrogen peroxide in methanol for 30 minutes. The microwave-oven heating was carried out with three 5-minute cycles in either 10 mM citrate buffer (pH 6.0) or Tris buffer (pH 9.0). Routine IHC staining was then conducted using the polymer immunocomplex method. To assess the immunospecificity of each antibody, either normal mouse or rabbit sera was used as negative control instead of primary antibodies. Assessments of each sample (the scoring of IHC features) were made by 3 observers (A. Y., T. M., and M. S) and then compared.

For evaluation of IHC findings, scoring of nuclear or cytoplasmic immunoreactivity for p53, HNF-1β, ARID1A, ERα, PR, vimentin, PTEN, PIK3CA, WT1, and LEFTY was performed, as described previously [21,22]. Briefly, the proportion of immunopositive cells among the total number of counted cells was

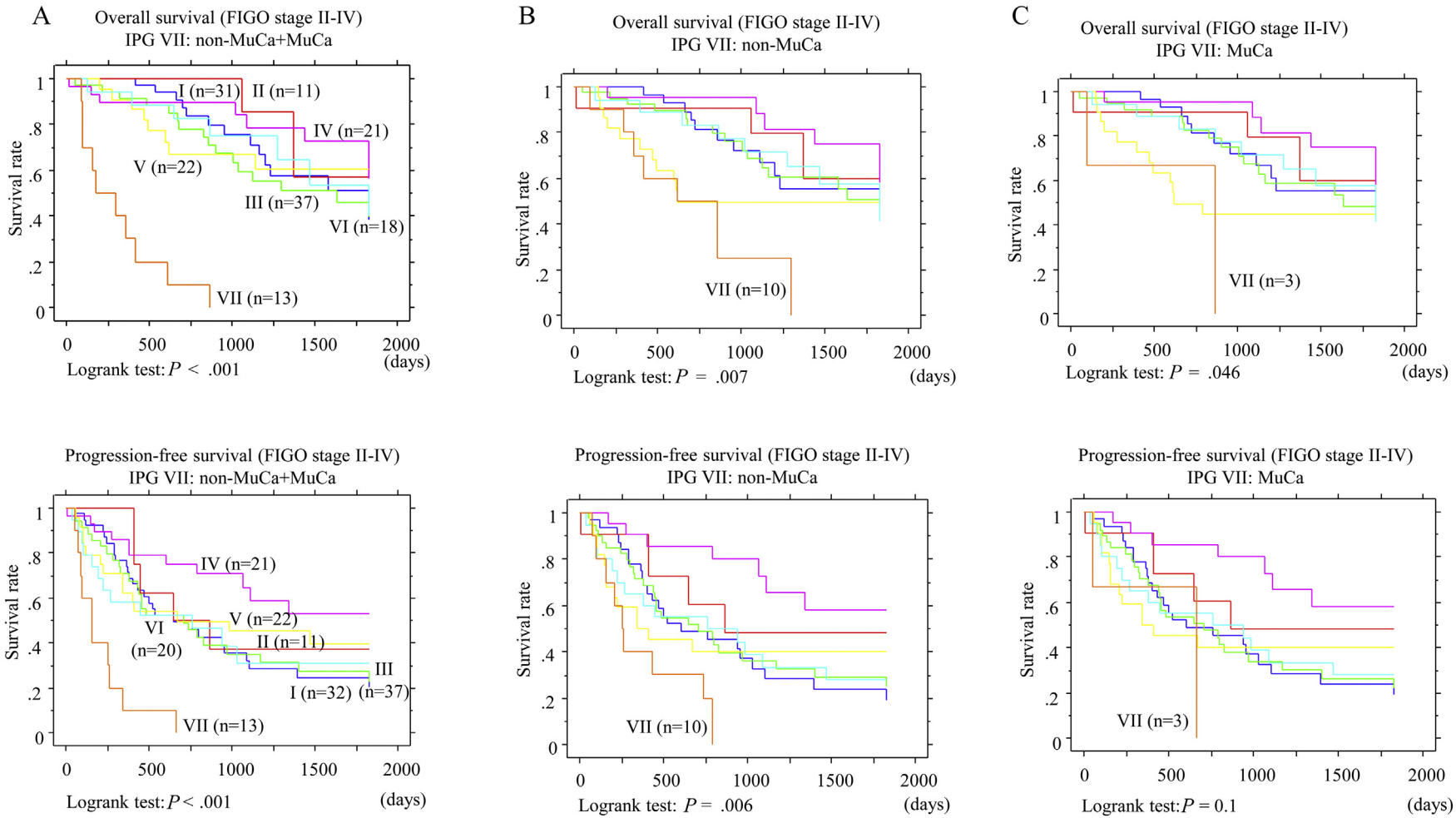

Fig. 6 Relationship of IPGs with OS and PFS in advanced OECas. OS (upper) and PFS (lower) of all patients with advanced OECa (A ;): patients with non-MuCa (B; HGSeCa and CCCa) and MuCa (C) in IPG VII as compared with those in IPGs I-VI. HGSeCa; MuCa, mucinous carcinoma; n, number of cases.;

subdivided into 5 categories as follows: 0, all negative; 1, <10%; 2, 10%-30%; 3, 30%-50%; and 4, >50% positive cells. The immunointensity was also subclassified into 4 groups: 0, negative; 1, weak; 2, moderate; and 3, strong immunointensity. IHC scores were generated by multiplication of the values of the 2 parameters. Nuclear immunopositivity for β-catenin and Ki-67 was also counted in at least 1000 cells in 5 randomly selected fields. Labeling indices (LIs) were then calculated as number per 100 cells, as described previously [21,22]. Cluster analyses for IHC data were also conducted by Ward method using R version 3.3.1 software (R Foundation for Statistical Computing, Vienna, Austria), on the basis of the colored expression level of each protein shown as red, orange, and green, which indicate relatively high (IHC scores or LIs > means + SDs), neutral (means ± SDs), and low (< mean − SDs) expression, respectively. To evaluate the prognostic significance of expression of the IHC markers, the scores or LIs were divided into 2 categories (high and low) with the mean values as the cutoff in each category.

2.4. Mutation analysis

A 10-μm paraffin wax section was reviewed, and carcinoma cell–rich areas were manually dissected under microscopic guidance while avoiding contamination by stromal components. Genomic DNA was extracted from 16 HGSeCas, 10 EmCas, 14 CCCas, 7 MuCas, and 8 HGCas using a QIAamp DNA FFPE Tissue kit (Qiagen, Hilden, Germany). Exons 5 to 9 of the *p53* gene, exon 3 of the *CTNNB* gene, exon 1 of the *k-ras*, and exons 9 and 20 of the *PIK3CA* gene were amplified by polymerase chain reaction, and the products were subsequently subjected to direct sequencing polymerase chain reaction as described previously [21-24].

2.5. Statistics

Comparative data were analyzed using the Mann-Whitney *U* test and χ^2 test, whichever was appropriate.

Overall survival (OS) was calculated as the time between onset and death or the date of the last follow-up evaluation. Progression-free survival (PFS) was also examined from the onset of treatment until relapse, disease progression, or last follow-up evaluation. OS and PFS were estimated using the Kaplan-Meier methods, and the statistical comparisons were made using the log-rank test. Univariate and multivariate analyses were performed using the Cox proportional hazards regression model. The cutoff for statistical significance was set as $P < .05$.

3. Results

3.1. Unsupervised cluster analysis of OECa by IHC findings

We performed IHC on 282 resected cases of OECa for 12 proteins, including p53, HNF-1β, ARID1A, ERα, PR,

Table 2 Univariate and multivariate analyses for OS and PFS in advanced ovarian carcinoma

Univariate analysis					Multivariate analysis				
Variables	Cutoff	Log-rank c2	*P*	Unfavorable factor	Variable	Cutoff	Hazard ratio	95% CI	*P*
OS					OS				
HNF-1β/p53/ARID1A	+++/others	17.6	<.0001	+++	HNF-1β/p53/ARID1A	+++/others	4.17	1.97-8.85	.0002
Age (y)	57/58	1.76	.18		FIGO stage	II/III IV	0.19	0.71-0.51	.001
FIGO stage	II/III V	25.66	<.0001	III-IV	Lymph node metastasis	−/+	0.93	0.48-1.84	.84
Tumor size (cm)	10.9/11.0	1.69	.19		Distant metastasis	−/+	0.50	0.27-0.93	.0276
Lymph node metastasis	−/+	14.06	.0002	+					
Distant metastasis	−/+	12.34	.0004	+					
PFS					PFS				
HNF-1β/p53/ARID1A	+++/others	10.5	.0012	+++	HNF-1β/p53/ARID1A	+++/others	2.875	1.50-5.52	.0015
Age (y)	57/58	0.81	.36		FIGO stage	II/III V	0.137	0.07-0.29	<.0001
FIGO stage	II/III V	42.91	<.0001	III-IV	Lymph node metastasis	−/+	1.345	0.81-2.24	.26
Tumor size	10.9/11.0	1.55	.21		Distant metastasis	−/+	0.462	0.27-0.78	.0037
Lymph node metastasis	−/+	17.13	<.0001	+					
Distant metastasis	−/+	20.54	<.0001	+					

NOTE. +++, HNF-1β+/p53+/ARID1A+.

vimentin, PTEN, PIK3CA, WT1, LEFTY, β-catenin, and Ki-67, which are considered to have significant power in the identification and classification of the tumors [21,25-27]. Representative IHC findings for these IHC markers in OECa are illustrated in Figs. 1 and 2. We observed significantly higher IHC scores or LIs for p53 or WT1 in HGSeCa and LGSeCa, HNF-1β and LEFTY in CCCa, and nuclear β-catenin, ERα, PR, and vimentin in EmCa, in contrast to significantly lower ARID1A, ERα, and PR scores in CCCa as compared with those in other histotypes. Relatively higher p53 and HNF-1β scores and lower PTEN score were also observed in MuCa. In contrast, changes in PIK3CA score and Ki-67 LI were relatively minor among the different histotypes of OECa (Supplementary Fig. S1).

Hierarchical clustering was then applied to the IHC data for each marker to determine whether the immunophenotypic features of OECa could be readily categorized (Fig. 3). Seven IPGs were revealed from this analysis, and the distribution of the HGSeCa, LGSeCa, EmCa, CCCa, MuCa, and HGCa cases present in each group is shown in Table 1. IPGs I and III contained a high proportion of HGSeCas, whereas IPGs V and VI included mostly CCCas. IPGs IV and VII were consisted predominantly of EmCas and MuCas. In addition, IPG II was relatively heterogeneous and contained a similar distribution of HGSeCas, EmCas, and MuCas.

It has been demonstrated that an HGSeCa-like profile shows *p53* mutations in the absence of EmCa-like mutations, the latter of which are defined as one or more mutations in the *CTNNB*, *PIK3CA*, or *k-ras* gene with or without a concurrent *p53* mutation [28,29]. To further examine associations among the protein expression, gene mutation status, and IPGs, a total of 55 OECa cases were selected from each of the IPG, and the mutation statuses of the *CTNNB*, *PIK3CA*, and *k-ras* genes were investigated (Supplementary Table S1). Alterations in the *CTNNB* and *p53*, but not *PIK3CA*, genes were significantly associated with their protein expression statuses (Supplementary Fig. S2). Mutations in the *CTNNB* gene were predominantly detected in EmCas and IPG IV relative to other histotypes and immunoprofiles, respectively, whereas alterations in the *p53* gene were frequently observed in HGSeCas, as well as IPGs II, III, and VII. *PIK3CA* gene abnormalities were predominant in HGSeCas and CCCas, as well as IPGs II, V, and VII, whereas *k-ras* gene mutations were not associated with either histotype or IPG (Supplementary Table S2).

As shown in Fig. 4, the p53 score was significantly higher in IPGs II, III, and VII, whereas HNF-1β and LEFTY scores were predominantly higher in IPGs V, VI, and VII as compared with those in other IPGs. On the other hand, both ERα and PR scores were significantly lower in IPGs V, VI, and VII. In addition, the ARID1A score was significantly lower in IPG V, whereas the WT1 score was higher in IPGs I and III. The IHC scores or LIs for other markers including vimentin, PTEN, PIK3CA, and Ki-67 were varied among the IPGs. Collectively, high HNF-1β scores were observed in IPGs V to VII categories, in contrast to the low scores in IPG I-IV categories. In the former categories, ARID1A score was low in IPG V, whereas a combination of high ARID1A and either low p53 or high p53 scores was observed in IPG VI and IPG VII, respectively. In the IPG I-IV categories, high and low p53 scores were found in IPGs II/III and IPGs I/IV, respectively. Moreover, WT1 scores were high in IPGs I and III, whereas its scores were low in IPGs II and IV. Based on these findings, we developed a simplified IHC-based panel to categorize OECa cases into IPGs I-VII using the 4 most correlative IHC markers including HNF-1β, p53, WT1, and ARID1A (Fig. 5).

3.2. Association between IPGs and prognosis in OECa

We next wanted to determine if the full-range IPGs that we had developed had any predictive values; thus, we analyzed the OS and PFS of 153 OECa cases of clinical stage II-IV with respect to the IPG. The Kaplan-Meier curves showed that the patients in IPG VII, which was composed of MuCa (57.7%), HGSeCa (23.1%), and CCCa (19.2%) cases, had more unfavorable OS and PSF as compared with those of other IPGs (Fig. 6A). Similar findings for both OS and PFS analyses were also observed in advanced OECa cases excluding HGCas (Supplementary Fig. S3). Because the patients with MuCa had the most unfavorable OS and PFS as compared with the other OECa histotypes (Supplementary Fig. S4) and the IPG VII included the most cases of MuCa, IPG VII was further subdivided into non-MuCa and MuCa cases. As shown in Fig. 5B, non-MuCa cases, including 6 HGSeCas and 4 CCCas (Supplementary Table S3), in IPG VII had equally unfavorable OS and PFS as the MuCa cases (Fig. 5C) relative to those in the other IPGs, demonstrating that the cases with the HNF-1β+/p53+/ARID1A+ immunophenotype had the most unfavorable prognosis regardless of histotype (Supplementary Fig. S5 and Supplementary Table S3).

As shown in Table 2, univariate Cox proportional hazards regression revealed that the HNF-1β+/p53+/ARID1A+ immunophenotype and clinical stage, lymph node status, and distant metastasis were significant prognostic factors for OS and PFS in OECa of clinical stages II-IV. Multivariate Cox regression analysis also showed that the HNF-1β+/p53+/ARID1A+ immunophenotype, clinical stage, and distant metastasis were significant and independent prognostic factors for OS and PFS in advanced OECa.

4. Discussion

The present study clearly provided evidence that histotype-independent classification of OECas by 12 IHC markers including p53, HNF-1β, ARID1A, ERα, PR, vimentin, PTEN, PIK3CA, WT1, LEFTY, β-catenin, and Ki-67, which are consistently expressed in the tumors [21,25-27], was useful for prognosis prediction. The immunophenotype of each IPG seemed to be also linked with several gene mutations including those in *p53*, *CTNNB*, and *PIK3CA*. However, IHC for 12 protein markers is not always feasible because some of the antibodies are not widely available, which precludes their implementation in

daily pathology practice. Based on the results of both hierarchical clustering analysis and the protein expression levels, we established a simplified categorization system of OECa tumors into 7 IPGs using the 4 most correlative IHC markers including p53, HNF-1β, ARID1A, and WT1.

Our results also demonstrated that although both IPGs I and III contained a high proportion of HGSeCas, the p53 scores were significantly different between the 2 groups despite the similar histopathologic phenotypes. Similar findings were also observed for the ARID1A scores of the CCCas categorized into IPGs V and VI. Given the findings showing that EmCa and MuCa were mainly categorized into IPGs IV and VII, respectively, it is suggested that both HGSeCa and CCCa may have more heterogeneous phenotypic characteristics as compared with them.

An important finding in this study was that the patients in IPG VII, which included HGSeCas, CCCas, and MuCas, had significantly worse OS and PFS than did those in other IPGs in advanced OECa cases. Moreover, the patients with non-MuCa (HGSeCa and CCCa), as well as MuCa, in IPG VII also had worse prognosis as compared with patients in IPGs III (HGSeCa), and IPGs V and VI (CCCa). Taken together, our findings suggested that the biological behavior of both HGSeCa and CCCa in IPG VII, but not those in IPG I, III, or V, may be more similar to that of MuCa, which was mainly categorized into IPG VII and showed the worst prognosis among the OECa subtypes. In addition, multivariate Cox regression analysis also showed that the HNF-1β+/p53 +/ARID1A+ immunophenotype and clinical stage were significant and independent prognostic factors for OS and PFS in advanced OECa. These findings suggest that the immunophenotype of the tumor cells may be more useful as prognostic and predictive parameters for OECa rather than histopathology-based classification.

It has been reported that combining 2 IHC labeling patterns associated with TP53 mutations (0% and 60%-100% positive cells) correctly identified a mutation in 94% of cases [30]. In our results, however, the Kaplan-Meier curves showed no significant differences in OS but were observed in PFS among the patients with negative p53 (score 0), low expression (score 1-5), and high expression (score >5), whereas the patients with high p53 scores (≧5) had worse OS and PFS as compared with those with low p53 scores (<5; Supplementary Fig. S6). At the present time, although we are unable to provide an appropriate explanation for the observation, it seems that our IPG system including p53 scoring may be useful to predict the prognosis in advanced OECas.

In general, functional p53 plays a central role in susceptibility to apoptosis, and its activation is critical for sensitivity to genotoxic agents like cis-diaminedichloro-platinum(II), cis-$[PtCl_2(NH_3)_2]$ (CDDP), whereas its loss can enhance resistance to chemotherapy [31,32]. HNF-1β has a drug resistance–related function through 4 pathways including ErbB signaling, focal adhesion, apoptosis, and p53 signaling [33]. Our previous study also demonstrated that an association between HNF-1β and NF-κB signaling may participate in cell survival by alteration of apoptotic events, particularly in mitochondria-mediated pathways, through upregulation of bcl2 expression in CCCa [34]. Given that ARID1A functions as a tumor suppressor gene [35], it seems that the combined increase in expression of HNF-1β and p53 may act as unfavorable prognostic factors of OECa in IPG VII. Further investigations into these points are clearly warranted.

In conclusion, we developed a categorization system that can readily classify OECa tumors into IPGs based on their immunophenotype and not their histotype and can facilitate prognostic prediction. Furthermore, our classification system can identify immunoprofiles using only 4 of the most correlative IHC markers, which can demonstrate the most unfavorable immunophenotype in the tumors, and thus facilitate prognostic prediction of OECa. Further large studies with the inclusion of additional clinicopathological variables and the control of case selection bias are clearly warranted to validate our findings.

Supplementary data

Supplementary data to this article can be found online at https://doi.org/10.1016/j.humpath.2018.10.036.

References

[1] Ushijima K. Current status of gynecologic cancer in Japan. J Gynecol Oncol 2009;20:67-71.
[2] Salani R, Backes FJ, Fung MF, Holschneider CH, Bristow LP, Goff BA. Posttreatment surveillance and diagnosis of recurrence in women with gynecologic malignancies: Society of Gynecologic Oncologists recommendations. Am J Obstet Gynecol 2011;204:466-78.
[3] Kobel M, Kalloger SE, Boyd N, et al. Ovarian carcinoma subtypes are different diseases: implications for biomarker studies. PLoS Med 2008; 5:e232.
[4] Kobel M, Kalloger SE, Huntsman DG, et al. Differences in tumor type in low-stage versus high-stage ovarian carcinomas. Int J Gynecol Pathol 2010;29:203-11.
[5] Wang V, Li C, Lin M, et al. Ovarian cancer is a heterogeneous disease. Cancer Genet Cytogenet 2005;161:170-3.
[6] du Bois A, Quinn M, Thigpen T, et al. 2004 Consensus statements on the management of ovarian cancer: final document of the 3rd International Gynecologic Cancer Intergroup Ovarian Cancer Consensus Conference (GCIG OCCC 2004). Ann Oncol 2005;16:567-76.
[7] Fehrmann RS, Li X-Y, van der Zee AG, et al. Profiling studies in ovarian cancer: a review. Oncologist 2007;12:960-6.
[8] An HJ, Kim DS, Park YK, et al. Comparative proteomics of ovarian epithelial tumors. J Proteome Res 2006;5:1082-90.
[9] Bengtsson S, Krogh M, Szigyarto CA, et al. Large-scale proteomics analysis of human ovarian cancer for biomarkers. J Proteome Res 2007;6: 1440-50.
[10] Young TW, Rosen DG, Mei FC, et al. Up-regulation of tumor susceptibility gene 101 conveys poor prognosis through suppression of p21 expression in ovarian cancer. Clin Cancer Res 2007;13:3848-54.
[11] Gortzak-Uzan L, Ignatchenko A, Evangelou AI, et al. A proteome resource of ovarian cancer ascites: integrated proteomic and bioinformatic analyses to identify putative biomarkers. J Proteome Res 2008;7:339-51.
[12] Fountain J, Trimble E, Birrer MJ. Summary and discussion of session recommendations. Gynecol Oncol 2006;103:S23-5.
[13] Kobel M, Kalloger SE, Baker PM, et al. Diagnosis of ovarian carcinoma cell type is highly reproducible: a transcanadian study. Am J Surg Pathol 2010;34:984-93.

[14] Cramer SF, Roth LM, Ulbright TM, et al. Evaluation of the reproducibility of the World Health Organization classification of common ovarian cancers. With emphasis on methodology. Arch Pathol Lab Med 1987;111:819-29.
[15] Hernandez E, Bhagavan BS, Parmley TH, Rosenshein NB. Interobserver variability in the interpretation of epithelial ovarian cancer. Gynecol Oncol 1984;17:117-23.
[16] Lund B, Thomsen HK, Olsen J. Reproducibility of histopathological evaluation in epithelial ovarian carcinomas. Clinical implication. APMIS 1991;99:353-8.
[17] Kobel M, Bak J, Bertelsen BI, et al. Ovarian carcinoma histotype determination is highly reproducible, and is improved through the use of immunohistochemistry. Histopathology 2014;64:1004-13.
[18] Kobel M, Kalloger SE, Carrick J, et al. A limited panel of immunomarkers can reliably distinguish between clear cell and high-grade serous carcinoma of the ovary. Am J Surg Pathol 2009;33:14-21.
[19] Longacre TA, Wells M, Bell DA, Malpica A, Prat J, Ronnet BM. Tumours of the tumours of the ovary. In: Kurman RJ, Carcangiu ML, Herrington CS, Young RH, editors. WHO Classification of Tumours of Female Reproductive Organs. Lyon: IARC; 2014. p. 11-86.
[20] Benedet JL, Bender H, Jones III H, Ngan Y, Pecorelli S. FIGO staging classifications and clinical practice guidelines in the management of gynecologic cancers. FIGO Committee on Gynecologic Oncology. Int J Gynaecol Obstet 2000;70:209-62.
[21] Akiya M, Yamazaki M, Matsumoto T, et al. Identification of LEFTY as a molecular marker for ovarian clear cell carcinoma. Oncotarget 2017;8:63646-64.
[22] Fei W, Kijima D, Hashimoto M, et al. A functional role of LEFTY during progesterone therapy for endometrial carcinoma. Cell Commun Signal 2017;15:56.
[23] Matsumoto T, Yamazaki M, Takahashi H, et al. Distinct *β-catenin* and *PIK3CA* mutation profiles in endometriosis-associated ovarian endometrioid and clear cell carcinomas. Am J Clin Pathol 2015;144:452-63.
[24] Yamashita K, Yoshida T, Shinoda H, Okayasu I. Novel method for simultaneous analysis of *p53* and *K-ras* mutations and p53 protein expression in single histologic sections. Arch Pathol Lab Med 2001;125:347-52.
[25] Goff BA, Ries JA, Els LP, Coltrera MD, Grown AM. Immunophenotype of ovarian cancer as predictor of clinical outcome: evaluation at primary surgery and second-look procedure. Gynecol Oncol 1998;70:378-85.
[26] Kallonger SE, Kobel M, Leung S, et al. Calculator for ovarian carcinoma subtype prediction. Mod Pathol 2011;24:512-21.
[27] Kspar HG, Crum CP. The utility of immunohistochemistry in the differential diagnosis of gynecologic disorders. Arch Pathol Lab Med 2015;139:39-54.
[28] Cancer Genome Atlas Research Network. Integrated genomic analyses of ovarian carcinoma. Nature 2011;474:609-15.
[29] McConechy MK, Ding J, Senz J, et al. Ovarian and endometrial endometrioid carcinomas have distinct *CTNNB1* and *PTEN* mutation profile. Mod Pathol 2014;27:128-34.
[30] Yemelyanova A, Vang R, Kshirsagar M, et al. Immunohistochemical staining patterns of p53 can serve as a surrogate marker for TP53 mutations in ovarian carcinomas: an immunohistochemical and nucleotide sequencing analysis. Mod Pathol 2011;24:1248-53.
[31] Reles A, Wen WH, Schmider A, et al. Correlation of *p53* mutations with resistance to platinum-based chemotherapy and shortened survival in ovarian cancer. Clin Cancer Res 2001;7:2984-97.
[32] Farrand L, Byun S, Kim JY, et al. Piceatannol enhances cisplatin sensitivity in ovarian cancer via modulation of p53, X-linked inhibitor of apoptosis protein (XIAP), and mitochondrial fission. J Biol Chem 2013;288:23740-50.
[33] Li J, Zhang Y, Gao Y, et al. Downregualtion of HNF1 homeobox B is associated with drug resistance in ovarian cancer. Oncol Rep 2014;32:979-88.
[34] Suzuki E, Kajita S, Takahashi H, Matsumoto T, Tsuruta T, Saegusa M. Transcriptional upregulation of HNF-1β by NF-κB in ovarian clear cell carcinoma modulates susceptibility to apoptosis through alteration in bcl-2 expression. Lab Invest 2015;95:962-72.
[35] Guan B, Wang TL, Shih leM. ARID1A, a factor that promotes formation of SWI/SNF-mediated chromatin remodeling, is a tumor suppressor in gynecologic cancers. Cancer Res 2011;71:6718-27.